APPENDIX E

Appl. No. 10/781,979
Filed: February 19, 2004
Attorney's Docket No. 045600/274147
Group Art Unit 1638
Examiner: Anne R. Kubelik

APPLIED AND ENVIRONMENTAL MICROBIOLOGY, Oct. 1997, p. 3978–3984 Vol. 63, No. 10
0099-2240/97/$04.00+0

Single-Site Mutations in the Conserved Alternating-Arginine Region Affect Ionic Channels Formed by CryIAa, a *Bacillus thuringiensis* Toxin†

J. L. SCHWARTZ,[1,2]* L. POTVIN,[1] X. J. CHEN,[3] R. BROUSSEAU,[1] R. LAPRADE,[2] AND D. H. DEAN[3]

Biotechnology Research Institute, National Research Council of Canada,[1] and Groupe de Recherche en Transport Membranaire, Université de Montréal,[2] Montreal, Quebec, Canada, and Department of Biochemistry, Ohio State University, Columbus, Ohio[3]

Received 26 March 1997/Accepted 17 July 1997

The role of the third domain of CryIAa, a *Bacillus thuringiensis* insecticidal toxin, in toxin-induced membrane permeabilization in a receptor-free environment was investigated. Planar lipid bilayer experiments were conducted with the parental toxin and five proteins obtained by site-directed mutagenesis in block 4, an arginine-rich, highly conserved region of the protein. Four mutants were constructed by replacing the first arginine in position 21 by a lysine (R521K), a glutamine (R521Q), a histidine (R521H), or a glutamic acid (R521E). A fifth mutant was obtained by replacing the fourth arginine by a lysine (R527K). Like CryIAa, the mutants formed cation-selective channels. A limited but significant reduction in channel conductance was observed for all mutants except R521H. The effect was more dramatic for the voltage dependence of the channels formed by R521K and R521Q, which was reversed compared to that of the parental toxin. This study provides the first direct evidence of a functional role for domain III in membrane permeabilization. Our results suggest that residues of the positive arginine face of block 4 interact with domain I, the putative pore-forming region of CryIAa.

The crystals produced by the Gram-positive bacterium *Bacillus thuringiensis* during sporulation contain a variety of proteins that are toxic to larvae from lepidopteran, dipteran, and coleopteran insects (14). At the molecular level, it is believed that pore-related increased permeabilization of the apical membrane of midgut target cells constitutes the decisive step which results in cellular ionic imbalance and ultimately cell death (10, 15, 16). CryIC toxin forms ion channels in live cells from the Sf9 (*Spodoptera frugiperda*) and the UCR-SE1a (*Spodoptera exigua*) cell lines (23, 25). This protein also partitions in receptor-free planar lipid bilayers (26). Several other Cry toxins form ion-selective pores in planar lipid bilayers: CryIAa (11), CryIAc (28, 29), CryIIIA (29), CryIIIB2 (30), and CryIIA (6). However, little is known about the pore formation process or about the biophysical properties of the channels, their regulation or their molecular architecture.

It has been proposed (5, 9) that activated *B. thuringiensis* toxins have two distinct functional domains: a toxicity region (the first half of the protein) and a binding region (its second half). Highly conserved amino acid tracts are found in the toxic region (blocks 1 and 2) and in the binding region (blocks 3, 4 and 5) (14). It is believed that these regions play an important role in the insecticidal activity of Cry toxins. Recently, structural data have been obtained by X-ray crystallography of CryIIIA, a coleopteran toxin (20), and CryIAa, a lepidopteran toxin (11). They show that the two toxins share a three-domain tertiary structure. Among the conserved blocks, block 2 is located mainly in domain I, which is thought to be involved in transmembrane channel formation. Block 2 includes α_7, the last helix of helix-rich domain I, and the flexible loop which links domain I to domain II. Two other conserved tracts, block 4 and block 5, are located in domain III, whose role is believed to be limited to the maintenance of the protein structural stability. In particular, the fifth conserved tract has been shown to be critical to the production of properly conformed CryIVA toxins but had no effect on their insecticidal activity (24). Block 4, which is part of β-sheet 17 of CryIAa, is of particular interest. This region of domain III, RYRVRIR (R, arginine; Y, tyrosine; V, valine and I, isoleucine) from position 521 to position 527, presents a strongly positively charged face and a highly hydrophobic face. It interacts intramolecularly with block 2 of domain I via a hydrogen bond between the side chain of the third arginine (position 525) and a carbonyl oxygen from the arginine in position 254 of block 2, with the latter being the first residue in the loop which links domain I and domain II (11).

Mutational studies were conducted on block 4 of CryIAa (3). Although mutations in the second and third arginine positions resulted in altered structure and expression of the protein, other mutations directed to the first or the fourth arginine provided products that were essentially similar to the wild-type toxin in structure, as assessed by trypsin susceptibility and circular dichroism spectra, and in binding to brush border membrane vesicles from silkworm (*Bombyx mori*) midguts. However, these mutants exhibited significant functional differences compared to CryIAa. In vivo toxicity to *B. mori* was reduced, and the mutants were substantially less effective in inhibiting the short-circuit currents recorded from voltage-clamped silkworm midguts (3). These results suggest that block 4 plays a role in postbinding events, particularly at the level of membrane permeabilization. Further work on these mutants has been conducted recently to determine their effect on *B. mori* brush border membrane vesicle permeability by using light-scattering detection of vesicle swelling (31). It supported

* Corresponding author. Mailing address: Biotechnology Research Institute, National Research Council of Canada, 6100 Royalmount Ave., Montreal, Quebec, Canada H4P 2R2. Phone: (514) 496-6355. Fax: (514) 496-6213. E-mail: jean-louis.schwartz@bri.nrc.ca.

† NRCC publication 49508.

the previous results of Chen et al. (3) and demonstrated that mutations in domain III do indeed affect CryIAa toxin function at the midgut membrane level.

In the present study we examined the role played by block 4 of domain III in CryIAa channel formation in receptor-free, artificial phospholipid membranes. By combining single-site mutagenesis in block 4, the conserved alternating-arginine segment of domain III, with functional studies using ion channel reconstitution into planar lipid bilayers, we demonstrated directly that domain III of CryIAa plays a role in membrane permeabilization induced by the toxin. More specifically, our results show that both the conductance and the voltage dependence of the toxin-mediated channels are sensitive to single-residue changes made in the conserved block 4 of domain III.

MATERIALS AND METHODS

Mutagenesis and toxin expression and preparation. Mutant genes (31) were expressed in *Escherichia coli* JM103 cells which were grown for 2 days. Inclusion bodies were prepared and solubilized in sodium carbonate buffer at pH 9.5. Toxins were obtained by trypsin digestion of protoxins at a final trypsin/protoxin ratio of 1:25 (wt/wt) for at least 4 h at 37°C. Small peptides were removed by column chromatography (fast protein liquid chromatography-Mono Q; Pharmacia Biotech, Piscataway, N.J.). Digested toxins were dialyzed overnight against sodium carbonate buffer and then examined by sodium dodecyl sulfate (10%)-polyacrylamide gel electrophoresis (17). For bilayer work, toxins were precipitated with 40% ammonium sulfate and resuspended in 150 mM KCl buffered with 25 mM Tris at pH 9.0 to prepare the toxin stock solution (0.8 to 1.5 mg of protein per ml). All chemicals were obtained from Sigma (St. Louis, Mo.), unless noted otherwise.

Planar lipid bilayer methods and data analysis. Planar lipid bilayers (26) were formed from a 7:2:1 lipid mixture (final concentration of 25 mg/ml in decane) of phosphatidylethanolamine, phosphatidylcholine, and cholesterol (Avanti Polar Lipids, Alabaster, Ala.). The bilayer was painted, using disposable glass rods made from prepulled, sealed-tip Pasteur pipettes, across a 250-μm orifice drilled in a Delrin cup (*cis* chamber) and pretreated with the above-described lipid mixture dissolved in chloroform. Membrane thinning was monitored by visual observation through a binocular dissection microscope and was assayed electrically by applying a triangular voltage to the membrane. Typical membrane capacitance values ranged between 150 and 250 pF. Channel activity following addition of trypsin-activated toxin or its mutants to the *cis* chamber at 5 to 20 μg/ml (85 to 340 nM) was monitored by step changes in the current recorded during holding test voltages across the planar lipid bilayer. Toxin incorporation was facilitated by stirring the buffer in the *cis* chamber with a magnetic stir bar and by applying a holding voltage of −80 mV. Temperature and pH were measured with a combined instrument (BAT-10/PHM-1) from Physitemp (Clifton, N.J.). All experiments were performed at room temperature (20 to 22°C) in buffer solutions containing either 150 or 450 mM KCl, 1 mM $CaCl_2$, and 10 mM Tris, pH 9.0. Single-channel currents were recorded with an Axopatch-1D patch-clamp amplifier (Axon Instruments, Foster City, Calif.). The 5-kHz low-pass-filtered currents were pulse-code modulated (Instrutech Corp., Great Neck, N.Y.) and stored on VHF magnetic tape. For analysis, data were played back through an analog eight-pole, low-pass Bessel filter (Frequency Devices, Haverhill, Mass.) set at 600 Hz and digitized at a 2.5-kHz sampling frequency (Labmaster TL-125; Axon Instruments). Data analysis was performed on a personal computer with pClamp or Axotape software (Axon Instruments). For each applied voltage, current amplitudes were measured on the recorded traces. For some voltages, current amplitude histograms were generated. Due to the multichannel nature of most records, no attempt was made to compare the kinetic properties of the single channels formed by the various proteins tested in this study, as multichannel activity rendered the interpretation of open-time and closed-time analyses quite complicated (21). However, a quantitative estimate of channel activity was obtained by measuring t_o, the sum of the total open times spent by the N identical channels at each open state level, over t_i, the total recording time interval. N, the number of active channels in the bilayer, was obtained from channel current amplitude histograms, and P_o, the estimated mean probability of a channel being open, was calculated by $P_o = (t_o/t_i)/N$.

Subconductance states were recognized as described before (26) by using the following identification criteria (7): (i) direct transitions from subconductance levels to main conductance levels were observed, (ii) subconductance states were never observed in the absence of the main conductance state, and (iii) the main conducting state did not result from the superposition of two or more independent channel openings.

Applied voltages are defined with respect to the *trans* chamber, which was held at virtual ground. Positive currents (i.e., currents flowing through the planar lipid bilayer from the *cis* chamber to the *trans* chamber) are shown as upward deflections. The direction of current flow corresponds to positive charge movement.

Conductance data are given as means ± standard errors of the means (SEMs).

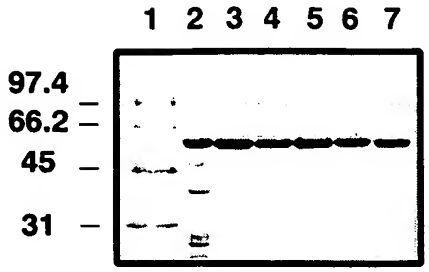

FIG. 1. Sodium dodecyl sulfate (10%)-polyacrylamide gel electrophoresis of trypsin-activated CryIAa and alternating-arginine mutant toxins. Lane 1, molecular size markers, with molecular masses (in kilodaltons) shown on the left; lane 2, R521E; lane 3, R521H; lane 4, R521K; lane 5, R521Q; lane 6, R527K; lane 7, CryIAa. The proteins were visualized by Coomassie brilliant blue staining.

The mean conductance of each mutant main conducting state was compared to that of the parental toxin by using a two-tailed Mann-Whitney U test ($P < 0.01$).

RESULTS

CryIAa and its mutants form channels in planar lipid bilayers. Figure 1 shows that the wild-type protoxin as well as the arginine mutants were processed by trypsin to approximately 62-kDa toxic cores. The recombinant CryIAa used in this study formed channels that resembled closely those recorded under similar conditions after incorporation of wild-type CryIAa toxin purified by fast protein liquid chromatography (11). Similarly, the products obtained from single-site mutations of arginine in position 521 or 527 of the toxin partitioned in lipid membranes after a few minutes and at similar doses (85 to 340 nM). Well-resolved current jumps corresponding to the passage of ions through open channels were recorded as illustrated in Fig. 2 (traces).

Channel activity: multiple channels and substates. Usually, the number of active channels following the incorporation of CryIAa or its mutants into the planar lipid bilayer increased for a short period of time (5 to 10 min). It then remained stable for tens of minutes to hours, suggesting that progressive but rather limited incorporation took place in the planar lipid bilayer. Depending on the protein, more than one level of current jumps were observed, and for some of them, bursts of up to 10 different levels were regularly recorded. Qualitative differences in toxin channel activity were apparent (Fig. 2, traces). Compared to that of CryIAa, R521H partition into the lipid bilayer was more difficult: at an equivalent dose, it took longer for the onset of channel activity, and usually only one principal conducting level was seen, with long open times separated by long closed times (1 s or longer). This mutant did possess small subconducting states at positive voltages (Fig. 2, traces). The kinetics of R521K and R527K channels was generally similar to that of CryIAa, with multiple, stable openings of average duration (1 s or less). Subconducting states were apparent in R527K held at positive voltages. Similarly, the channels formed by R521E possessed several subconducting states when positively polarized. In contrast, R521Q subconducting states were observed only at negative voltages. This protein displayed a noisier activity under these conditions.

Site-directed mutations affect single-channel conductance, voltage dependence, and activity level of CryIAa channels. Single-channel conductances of CryIAa and its mutants were derived from the slopes of linear regression curves of single-channel current data recorded for several voltages applied across the lipid bilayer (I-V curves). For conductance determination, only the principal conducting states, i.e., the largest

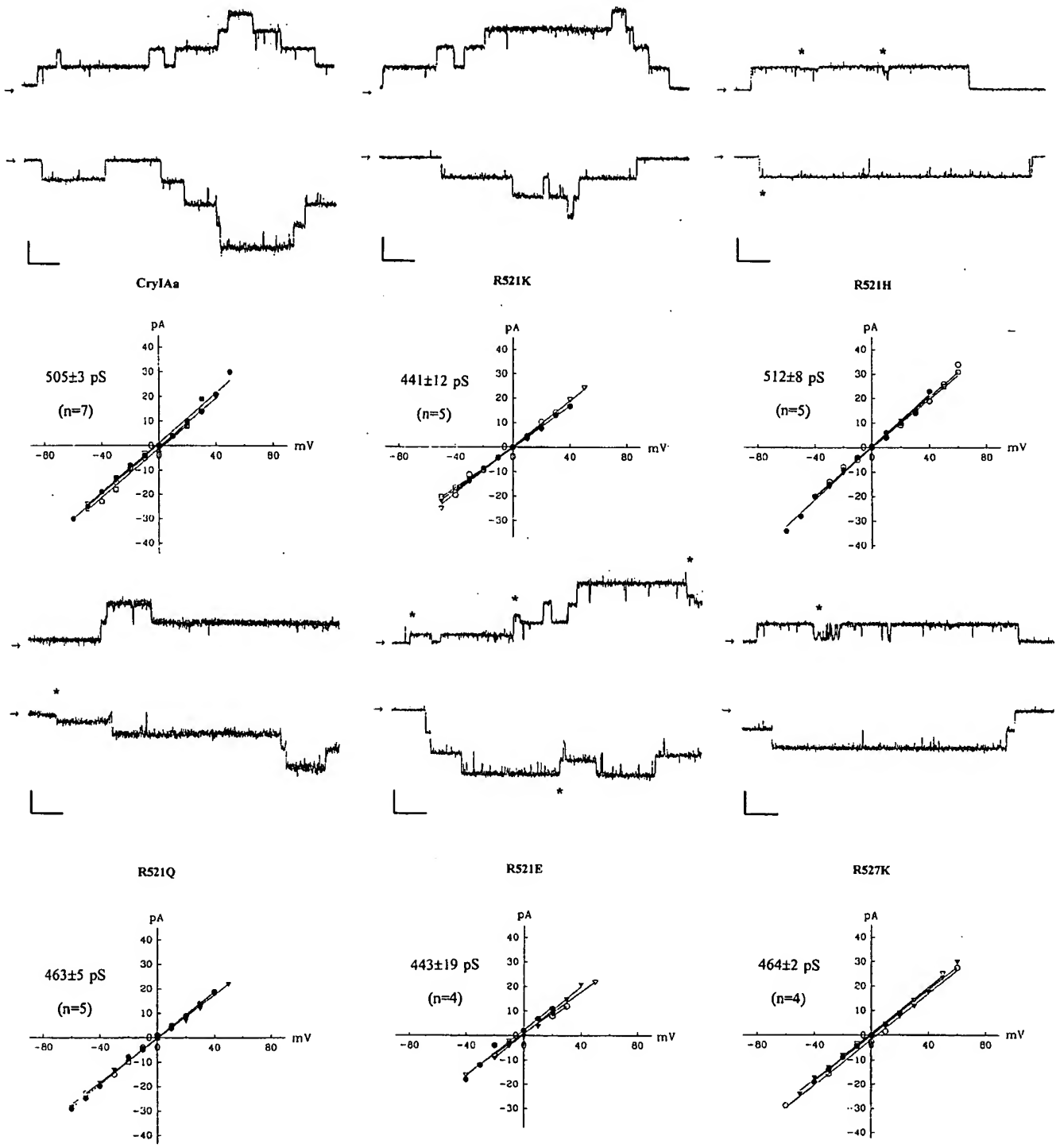

FIG. 2. The top parts of the panels show representative single-channel current traces recorded after partition of CryIAa and the five CryIAa mutants into planar lipid bilayers separating symmetrical KCl buffer solutions (150 mM in the *cis* chamber and 150 mM in the *trans* chamber) at pH 9.0. R521 mutants are shown in order of the charge shift sequence from positive to negative (R, K, H, Q, E). For the top traces, the applied voltage was +20 mV; for the bottom traces, the applied voltage was −20 mV. Arrows on the left of the traces indicate the closed state of the channels. Subconducting states are indicated by asterisks near the current traces. Scales: vertical bars, 10 pA; horizontal bars, 160 ms. The bottom parts of the panels show corresponding current-voltage relations (I-V curves). Data points from each individual experiment are represented by identical symbol types and were fitted by linear regression. Conductance values given in the upper left quadrants of the I-V curve graphs are means ± SEMs of the linear regression slopes.

TABLE 1. Single-channel properties and in vivo toxicities of wild-type CryIAa and five alternating-arginine mutants[a]

Activated toxin	Ion channel[b]			LD_{50} (ng/larva) (40–50 larvae)[c]
	Conductance (pS) (mean ± SEM)[d]	Mean P_o at:		
		−20 mV	+20 mV	
CryIAa	505.1 ± 2.5 (7)	0.37	0.25	4.5
R521H	512.2 ± 8.3 (5)	0.05	0.13	7.9
R521Q	463.4 ± 4.8[e] (5)	0.13	0.44	8.4
R521E	443.0 ± 19.2[e] (4)	0.62	0.38	8.4
R521K	441.2 ± 11.9[e] (5)	0.24	0.53	7.6
R527K	463.7 ± 2.2[e] (4)	0.04	0.06	7.7

[a] Conductance values of the R521 mutants are shown in decreasing order. This sequence differs from the charge shift sequence (R, K > H, Q > E) predicted for the 14-residue segment (PLSQRYRVRIRYAS) that includes the alternating-arginine region of block 4.

[b] With 5 to 20 μg of activated toxin per ml in the *cis* chamber and symmetrical (150 mM) KCl conditions.

[c] LD_{50}, 50% lethal dose. Results are reproduced from reference 31. Larvae were force fed 2 μl of activated toxin solution.

[d] The number of experiments for each toxin is shown in parentheses.

[e] Significantly different from CryIAa conductance by Mann-Whitney U test ($P < 0.01$).

detectable current jumps for which direct transitions between the baseline and the conducting level, could be observed, were considered. Such I-V curves were obtained from current data recorded under symmetrical ionic conditions (Fig. 2) and under nonsymmetrical conditions (see Fig. 4). The I-V curves were rectilinear, which indicated that the channels passed current equally well in either direction. Conductance data obtained with 150 mM KCl in both the *cis* and the *trans* chambers are listed in Table 1. Replacement of R521 by a histidine did not affect channel conductance, but the channel conductances of the other mutants were significantly reduced, by 8.1 to 12.7%. With 450 mM KCl in the *cis* chamber and 150 mM KCl in the *trans* chamber, the conductance of CryIAa was 575 ± 53 pS ($n = 2$), the conductance of R521K was 540 ± 29 pS ($n = 3$), and the conductance of R527K was 654 ± 18 pS ($n = 2$).

All-point amplitude histograms were generated from 30-s, 600-Hz filtered current records for each protein held at −20 or +20 mV (Fig. 3). They provided a semianalytical tool (4, 21) which was used to compare CryIAa to its mutated counterparts. The number of distinguishable peaks observed in such histograms indicated the presence of multiple channels or subconductance states (or both). The area under each peak represents the occupancy probability of the channels at each specific current level. Overall channel dependence on voltage can be qualitatively assessed by means of these histograms, as voltage-independent channels exhibit similar current peak distributions, particularly at voltages of opposite polarity. Figure 3 shows that for most toxins, amplitude histograms generated at −20 mV were different from those generated at +20 mV, a clear indication that the channels formed by CryIAa and most of the mutated toxins were voltage dependent. Furthermore, the amplitude histograms of channels formed by CryIAa and the arginine mutants were markedly different. At +20 mV, CryIAa displayed several distinct, equidistant peaks. The amplitude of the leftmost peak, which corresponded to the closed state of all channels, was the largest. The next peaks were progressively smaller. At −20 mV, the amplitude histogram of CryIAa was different: the closed state was less frequent, as demonstrated by the small amplitude of the rightmost peak, and occupancy of the second and third levels was favored. Therefore, the mean probability of CryIAa channels being open was increased by negative voltage. A similar behavior was observed for R521E. In contrast, the situation was reversed for R521K and R521Q, for which the occupancy probability shifted to higher current levels with positive voltages. Finally, R521H and R527K amplitude histograms reflected the low level of activity of these two mutants. This may be explained by the fact that the mutated proteins were difficult to incorporate into planar lipid bilayers. Alternatively, it is also possible that these particular mutations affected the gating of the proteins in such a way that the channels they formed remained mostly closed. P_o, the mean probability of each mutant channel being open at two opposite voltages, was obtained from typical 30- to 90-s current records (Table 1). These data are consistent with the results of the amplitude histogram analysis described above. They show that in contrast to CryIAa and R521E, R521K and R521Q were activated by positive voltages.

Like those of CryIAa, the channels formed by the mutants are cation selective. Ionic selectivity was tested under nonsymmetrical ionic conditions (450 mM KCl in the *cis* chamber and 150 mM KCl in the *trans* chamber). The current-voltage relations of CryIAa and its mutants were determined as described above. They shifted to the left, with zero-current voltages, i.e., reversal potential becoming more negative by approximately 25 mV for CryIAa, 15 mV for R521K, and 18 mV for R527K, as illustrated in Fig. 4. The other mutants behaved the same way (not shown). This shift was consistent with a Nernst equilibrium potential of −27.7 mV calculated for monovalent cations under these conditions, demonstrating the selectivity of the channels for cations. It should be noted that the apparent reduction of selectivity for cations, compared to that of CryIAa, was observed in a small set of experiments. Determination of whether it reflects a true effect of mutation needs further investigation.

DISCUSSION

In this study, the lipid bilayer technique was used to compare the in vitro ion transport properties of wild-type CryIAa toxin to those of five proteins obtained by site-directed mutagenesis in the conserved alternating-arginine region of CryIAa. Two important biophysical properties of the channels were significantly altered by mutations in block 4 of the third domain of CryIAa: the conductance of most mutants was reduced and the voltage dependence of two of them, R521K and R521Q, was reversed, compared to those of the wild-type toxin. While this effect of mutation on conductance was not dramatic, it was statistically significant. In terms of residue substitution in position 521 of the protein, the order of conductances (from the largest to the smallest) was H, Q, E, K. This order did not follow that of a progressive charge shift from positive to negative predicted for the residue sequence that maps CryIAa conserved block 4. Interestingly, R521K, the most conservative mutation, and R521E, the least conservative mutation, affected similarly the conductance of the channel, while a histidine substitution had no effect. These results suggest that local charges in the alternating-arginine region are at best a minor determinant of CryIAa conductance. The second major effect of arginine mutation, i.e., reversal of the channel voltage dependence, was clearly apparent in the all-point amplitude histograms constructed for CryIAa and its alternating-arginine mutants and was confirmed by the results of P_o analysis. Therefore, while the voltage dependence of CryIAa channels was influenced by certain mutations in block 4, it did not appear to be regulated by the charge of the residue in position 521. Other factors, like residue size, side chain orientation and intra- or intermolecular interactions, may also play a critical role. It is

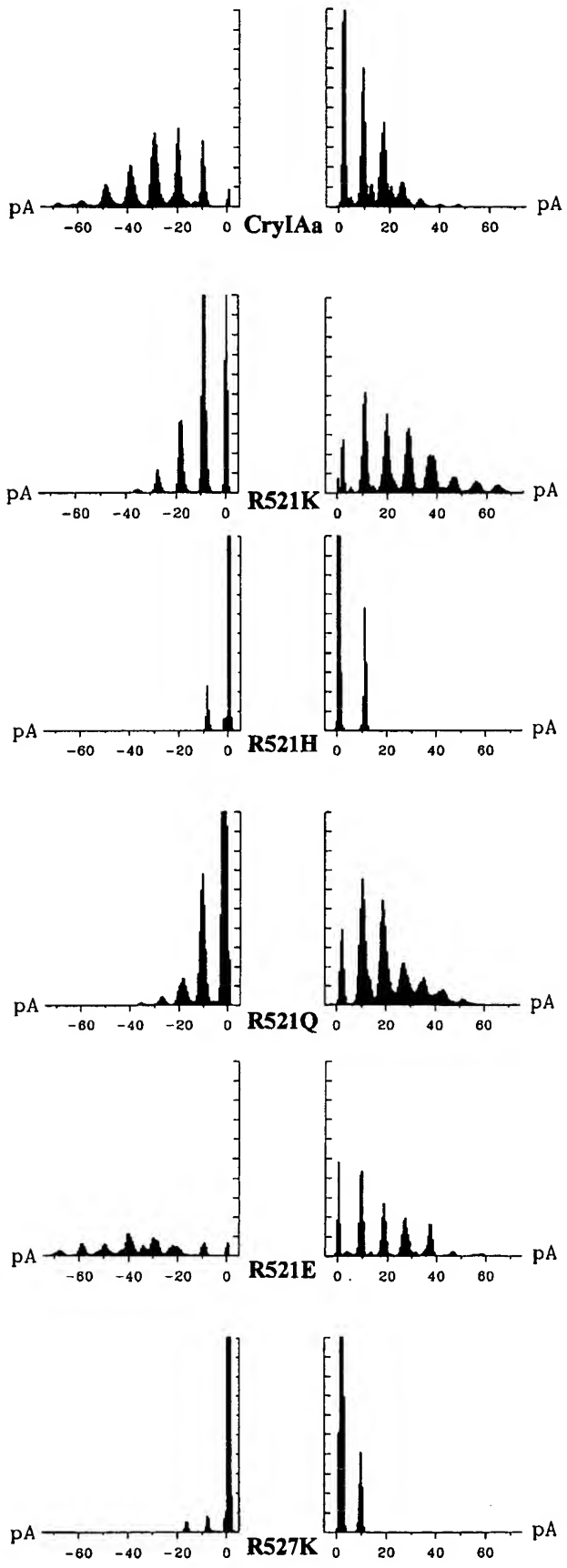

clear that further work is needed to clarify the complex nature of conductance and voltage regulation of Cry toxin channels.

Chen et al. (3) reported that arginine mutations in the fourth conserved block of CryIAa did not affect binding to *B. mori* brush border membrane vesicles. Compared to CryIAa, the mutants were approximately four times less active against second-instar silkworm larvae, as determined by diet surface contamination bioassays, and were less efficient in inhibiting the voltage clamp short-circuit current related to active transport across fifth-instar larvae midguts. Biological activity of the same mutated products as those used in the present investigation was tested with *B. mori* larvae by using a force-feeding bioassay (18). The results, which were reported elsewhere (31), are reproduced in Table 1 for convenient comparison with electrophysiological data. They show that compared to that of CryIAa, the toxicity of the mutants, i.e., the inverse of the 50% lethal dose, was reduced by 41 to 46%. In the same work (31), it was shown, using a light-scattering permeability assay on brush border membrane vesicles, that R521H, R521K, and R521Q exhibited the same membrane permeabilization capability as CryIAa, while R521E, R523K, R527H, and R527K were less active in the vesicle permeabilization assay. Our conductance data for R521E, R521H, and R527K are consistent with the light-scattering results. However, the mutants with lysine and glutamine in position 521 behaved differently in the two assays. The reasons for these discrepancies are not apparent, but they may be dependent on experimental conditions. It should be noted that both Chen et al. (3) and Wolfersberger et al. (31) conducted their experiments on biological preparations with functional CryIAa receptors. The results suggested that a change in ion transport properties of the mutated toxins took place, and it was concluded that mutations in the alternating-arginine region of CryIAa affected mainly the postbinding events related to toxicity. However, none of these studies could conclusively attribute the effect to altered pore function. In midgut voltage clamp experiments it is difficult to rule out metabolic pathways or paracellular permeabilities. Data from brush border membrane vesicle experiments report only the effects of toxins on membranes extracted from the luminal side of the midgut epithelium cell layer and in the absence of metabolic regulation. Furthermore, information obtained from these two experimental models is restricted to overall macroscopic ion transport, i.e., to the current whose total amplitude corresponds to the product of single-channel current amplitude, total number of channels present in the membrane, and probability of each channel being open (13).

Many of these interpretative difficulties can be reduced with the lipid bilayer approach, which provides direct biophysical information on single-channel properties of pore-forming proteins. Conductance, ionic selectivity, and, in the simplest cases, kinetic behavior can be ascribed precisely to the permeating pathway. On the other hand, the lipid bilayer technique also has its limitations: the artificial membrane may poorly mimic the actual membrane composition and environment in the gut, and of course there is no receptor and no metabolic regulation. Nevertheless, the present study demonstrates clearly that single-site mutations in block 4 of CryIAa resulted in altered

FIG. 3. All-point current amplitude histograms for 30-s recordings at −20 mV (left) and at +20 mV (right). R521 mutants are shown in order of the charge shift sequence from positive to negative (R, K, H, Q, E). Counts were distributed in 120 bins. They are shown on the vertical axes (4,000 counts/tick). Horizontal axes represent the current amplitude (pA). The rightmost peaks in the histograms on the left and the leftmost peaks in the histograms on the right correspond to the closed state of the channels at holding voltages.

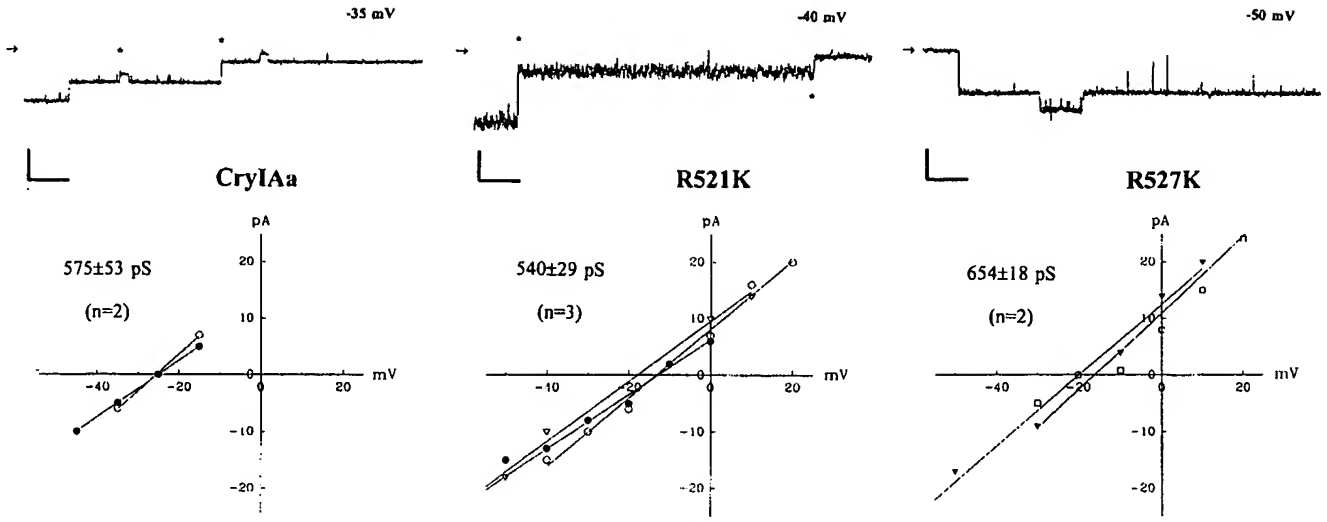

FIG. 4. The top parts of the panels show representative single-channel current traces recorded after partition of CryIAa and two R-to-K mutants into planar lipid bilayers separating nonsymmetrical KCl buffer solutions (450 mM in the *cis* chamber and 150 mM in the *trans* chamber) at pH 9.0. Applied voltages are indicated next to the traces. Arrows on the left of the traces indicate the closed state of the channels. Subconducting states are indicated by asterisks near the current traces. Scales: vertical bars, 10 pA; horizontal bars, 160 ms. The bottom parts of the panels show corresponding current-voltage relations. Data points from each individual experiment are represented by identical symbol types and were fitted by linear regression. Conductance values given in the upper left quadrants of the I-V curve graphs are means ± SEMs of the linear regression slopes. The direction and the magnitude of the reversal potential shifts (horizontal axis intercept) observed on the I-V curves demonstrate that CryIAa (−25.0 ± 1.1 mV), R521K (−14.7 ± 2.2 mV), and R527K (−18.2 ± 1.9 mV) are selective to cations.

functional properties of the protein. While all mutants retained the ability to partition into phospholipid membranes, R521H was significantly less effective in doing so, as only one channel opening level was usually observed. Furthermore, other crucial functions, such as conductance and voltage dependence, were affected by mutation. Considering that domain I of CryIAa, which is totally α-helical (11), is a leading candidate for pore formation, this study suggests that there are long-range interactions between domain I and the conserved alternating-arginine region of domain III and that these interactions do not depend solely on the charges of the mutated residues.

It has been proposed that Cry toxin insertion into membranes would be the result of "penknife"- or "umbrella"-like conformational changes triggered by binding of the toxin to its receptor (15). In the first model, the hairpin made of helices α_5 and α_6 flips into the cell membrane, and the rest of the molecule remains in the aqueous phase in a relatively unchanged conformation. In the second model, helices α_4 and α_5 enter the bilayer as a helical hairpin, and the other five helices of domain I flatten out on the membrane surface. An interesting feature of the umbrella model is that the region of the toxin that includes the alternating arginine segment moves closer to the area which could form the mouth of the putative channel formed by oligomeric association of other similarly unfolded toxins. Based on the data presented in this study and on the results of experiments conducted with disulfide-bridge-engineered Cry toxins (27, 32), it is tempting to propose that the alternating arginine region does indeed become part of, or interacts with, the mouth of the channel. Mutations in this region may therefore alter the channel mouth environment, which would result in reduced ion transport across the membrane and diminished biological activity.

In summary, this study demonstrates directly, and for the first time, that domain III, a part of the protein which has already been shown to play a role in binding and specificity determination (1, 2, 8, 19, 22), plays an important role in membrane permeabilization. More specifically, CryIAa toxin channel conductance and voltage dependence were significantly influenced by the alternating arginine segment of domain III. Furthermore, if the toxin pore is indeed formed by domain I, as has been proposed (11, 20), this study would also provide new direct evidence of a functional interaction between domain I and domain III in Cry toxins. Such an interaction between the N- and C-terminal regions of CryIAb has been implied at the level of toxin specificity (12). By providing new information on structure-function relations in CryIAa, this study will help to further our understanding of the molecular properties and the mode of action of *B. thuringiensis* toxins.

ACKNOWLEDGMENTS

This work was supported in part by grant OGP0171373 from the Natural Sciences and Engineering Research Council of Canada to R.L. and J.L.S. and by grant R01 AI29092 from the National Institutes of Health to D.H.D.

We thank A. Mazza, Biotechnology Research Institute, National Research Council of Canada, for expert technical assistance; P. Brink, State University of New York, Stony Brook, for stimulating suggestions on multiple-channel analysis; and P. Grochulski and L. Masson, Biotechnology Research Institute, National Research Council of Canada, for many helpful observations and valuable discussions.

REFERENCES

1. **Aronson, A. I., D. Wu, and C. Zhang.** 1995. Mutagenesis of specificity and toxicity regions of a *Bacillus thuringiensis* protoxin gene. J. Bacteriol. **177**: 4059–4075.
2. **Bosch, D., B. Schipper, H. Van der Kleij, R. A. De Maagd, and W. J. Stiekema.** 1994. Recombinant *Bacillus thuringiensis* crystal proteins with new properties: possibilities for resistance management. Bio/Technology **12**:915–918.
3. **Chen, X. J., M. K. Lee, and D. H. Dean.** 1993. Site-directed mutations in a highly conserved region of *Bacillus thuringiensis* δ-endotoxin affect inhibition of short circuit current across *Bombyx mori* midguts. Proc. Natl. Acad. Sci. USA **90**:9041–9045.
4. **Colquhoun, D., and F. J. Sigworth.** 1983. Fitting and statistical analysis of single-channel records, p. 191–263. *In* B. Sakmann and E. Neher (ed.), Single-channel recording. Plenum Press, New York, N.Y.
5. **Convents, D., C. Houssier, I. Lasters, and M. Lauwereys.** 1990. The *Bacillus thuringiensis* δ-endotoxin: evidence for a two domain structure of the minimal toxic fragment. J. Biol. Chem. **265**:1369–1375.
6. **English, L., H. L. Robbins, M. A. von Tersch, C. A. Kulesza, D. Ave, D. Coyle,**

C. S. Jany, and S. L. Slatin. 1994. Mode of action of CryIIA: a *Bacillus thuringiensis* delta-endotoxin. Insect Biochem. Mol. Biol. 24:1025–1035.
7. Fox, J. A. 1987. Ion channel subconductance states. J. Membr. Biol. 97:1–8.
8. Ge, A. Z., D. Rivers, R. Milne, and D. H. Dean. 1991. Functional domains of *Bacillus thuringiensis* insecticidal crystal proteins. J. Biol. Chem. 266:17954–17958.
9. Geiser, M., S. Schweitzer, and C. Grimm. 1986. The hypervariable region in the genes coding for entomopathogenic crystal proteins of *Bacillus thuringiensis*: nucleotide sequence of the *kurhd1* gene of subsp. *kurstaki* HD1. Gene 48:109–118.
10. Gill, S. S., E. A. Cowles, and P. V. Pietrantonio. 1992. The mode of action of *Bacillus thuringiensis* endotoxins. Annu. Rev. Entomol. 37:615–636.
11. Grochulski, P., L. Masson, S. Borisova, M. Pusztai-Carey, J. L. Schwartz, R. Brousseau, and M. Cygler M. 1995. *Bacillus thuringiensis* CrylA(a) insecticidal toxin: crystal structure and channel formation. J. Mol. Biol. 254:447–464.
12. Haider, M. Z., and D. J. Ellar. 1989. Functional mapping of an entomocidal δ-endotoxin. Single amino acid changes produced by site-directed mutagenesis influence toxicity and specificity of the protein. J. Mol. Biol. 208:183–194.
13. Hille, B. 1992. Ionic channels of excitable membranes, 2nd ed., p. 315–336. Sinauer Associates Inc., Sunderland, Mass.
14. Höfte, H., and H. R. Whiteley. 1989. Insecticidal crystal proteins of *Bacillus thuringiensis*. Microbiol. Rev. 53:242–255.
15. Knowles, B. H. 1994. Mechanism of action of *Bacillus thuringiensis* insecticidal δ-endotoxins. Adv. Insect Physiol. 24:275–308.
16. Knowles, B. H., and J. A. T. Dow. 1993. The crystal δ-endotoxins of *Bacillus thuringiensis*: models for their mechanism of action on the insect gut. Bioessays 15:469–476.
17. Laemmli, U. K., and M. Favre. 1973. Maturation of the head of bacteriophage T4. I. DNA packaging events. J. Mol. Biol. 80:575–599.
18. Lee, M. K., R. E. Milne, A. Z. Ge, and D. H. Dean. 1992. Domain III exchanges of *Bacillus thuringiensis* CrylA toxins affect binding to different gypsy moth midgut receptors. J. Biol. Chem. 267:3115–3121.
19. Lee, M. K., B. A. Young, and D. H. Dean. 1995. Location of a *Bombyx mori* receptor binding region on a *Bacillus thuringiensis* δ-endotoxin. Biochem. Biophys. Res. Commun. 216:306–312.
20. Li, J., J. Carroll, and D. J. Ellar. 1991. Crystal structure of insecticidal δ-endotoxin from *Bacillus thuringiensis* at 2.5 Å resolution. Nature 353:815–821.
21. Manivannan, K., S. V. Ramanan, R. T. Mathias, and P. R. Brink. 1992. Multichannel recordings from membranes which contain gap junction. Biophys. J. 61:216–227.
22. Masson, L., A. Mazza, L. Gringorten, D. Baines, V. Aneliunas, and R. Brousseau. 1994. Kinetics of *Bacillus thuringiensis* toxin binding with brush border membrane vesicles from susceptible and resistant larvae of *Plutella xylostella*. Mol. Microbiol. 14:851–860.
23. Monette, R., D. Savaria, L. Masson, R. Brousseau, and J. L. Schwartz. 1994. Calcium-activated potassium channels in the UCR-SE-1a lepidopteran cell line from the beet armyworm (*Spodoptera exigua*). J. Insect Physiol. 40:273–282.
24. Nishimoto, T., H. Yoshisue, K. Ihara, H. Sakai, and T. Komano. 1994. Functional analysis of block 5, one of the highly conserved amino acid sequences in the 130-kDa CryIVA protein produced by *Bacillus thuringiensis* subsp. *israelensis*. FEBS Lett. 348:249–254.
25. Schwartz, J. L., L. Garneau, L. Masson, and R. Brousseau. 1991. Early response of cultured lepidopteran cells to exposure to δ-endotoxin from *Bacillus thuringiensis*: involvement of calcium and anionic channels. Biochim. Biophys. Acta 1065:250–260.
26. Schwartz, J. L., L. Garneau, D. Savaria, L. Masson, and R. Brousseau. 1993. Lepidopteran-specific crystal toxins from *Bacillus thuringiensis* form cation- and anion-selective channels in planar lipid bilayers. J. Membr. Biol. 132: 53–62.
27. Schwartz, J. L., M. Juteau, P. Grochulski, M. Cygler, G. Préfontaine, R. Laprade, R. Brousseau, and L. Masson. 1997. Restriction of intramolecular movements within Cry1Aa toxin molecule of *Bacillus thuringiensis* by disulphide bond engineering. FEBS Lett. 410:397–402.
28. Schwartz, J. L., L. Potvin, J. Laflamme, A. Mazza, L. Masson, R. Brousseau, and R. Laprade. 1994. Effect of single site mutations on ionic channels formed by CrylA(c) *Bacillus thuringiensis* (*B. thuringiensis*) toxin. Biophys. J. 66:A221.
29. Slatin, S. L., C. K. Abrams, and L. English. 1990. Delta-endotoxins form cation-selective channels in planar lipid bilayers. Biochem. Biophys. Res. Commun. 169:765–772.
30. Von Tersch, M. A., S. L. Slatin, C. A. Kulesza, and L. H. English. 1994. Membrane-permeabilizing activities of *Bacillus thuringiensis* coleopteran-active toxin CryIIIB2 and CryIIIB2 domain I peptide. Appl. Environ. Microbiol. 60:3711–3717.
31. Wolfersberger, M. G., X. J. Chen, and D. H. Dean. 1996. Site-directed mutations in the third domain of *Bacillus thuringiensis* delta-endotoxin CrylAa affect its ability to increase the permeability of *Bombyx mori* midgut brush border membrane vesicles. Appl. Environ. Microbiol. 62:279–282.
32. Wu, S. J., O. Alzate, B. J. Honoelle, W. J. Becktel, and D. H. Dean. Protein engineering of *Bacillus thuringiensis* δ-endotoxins: disulphide mutants in domain I of Cry3A increase stability with no loss of toxicity. Submitted for publication.